Observation of Cumulative Spatial Focusing of Atoms

Windell H. Oskay,* Daniel A. Steck,† and Mark G. Raizen‡

Center for Nonlinear Dynamics and Department of Physics, The University of Texas at Austin, Austin, Texas 78712-1081

(Received 8 July 2002; published 26 December 2002)

We report an experimental study of the spatial distribution of ultracold cesium atoms exposed to a series of kicks from a standing wave of light. We observe cumulative focusing, leading to a spatial array of atoms which is of interest for atomic lithography. To observe the spatial distribution, we developed a free-space measurement technique that enables the reconstruction of the atomic motion as a function of time. We find increased focusing of atoms after as many as ten kicks, and the results are in good agreement with theoretical predictions.

DOI: 10.1103/PhysRevLett.89.283001 PACS numbers: 32.80.Pj, 42.50.Vk

The possibility of using light forces to control the deposition of atoms on surfaces is the basis for the emerging field of atom lithography. Interfering laser beams can focus atoms into very small regions as they deposit, thereby building nanostructures on a surface. The appeal of this method is massive parallelism, allowing simultaneous deposition over a large area. The basic implementation is to use a standing wave of light that is positioned close to a surface. Atoms are channeled by the optical dipole force as they approach the surface, and are thereby focused into parallel lines spaced by half a wavelength of the light. This method was first demonstrated with sodium [1] and, subsequently, with chromium [2,3] and aluminum [4]. The latter were chosen because they can be laser cooled and for their mechanical and chemical stability on surfaces. Laser focusing of atoms has subsequently been demonstrated in two dimensions and in a number of different experimental schemes [5–7].

Along with the successes of this program have come new technical challenges. While most atoms are focused, others are typically dispersed by the potential, leading to a uniform background of atoms in addition to the desired structure. The background can be comparable in thickness to the size of the nanoscale structures and therefore cannot easily be etched away without affecting the desired pattern [8]. This complicates the process of forming isolated structures on the surface, a necessary step for many nanoscale science applications. Focusing is usually achieved in one long interaction with the channeling standing wave, placed very close to the surface. This requires strong optical dipole potentials that can be realized only with a few atomic species. Many interesting materials do not have transitions that are easily accessible and also do not have cycling transitions. The requirement of strong focusing has thus limited the applications of atom lithography. One alternative approach is the method of standing-wave quenching, based on spatially dependent optical pumping of a metastable noble gas atom, and selective damaging of an organic resist [9]. This approach does not enable direct deposition on surfaces and may be limited by diffraction of the pattern before it reaches the surface.

We report in this Letter the experimental realization of a new approach that may extend the capabilities of atom lithography: We use time-dependent (or space-dependent for a beam) optical dipole potentials to focus atomic motion into periodic structures with a suppressed background. The basic idea, due to Averbukh and Arvieu [10,11], is to consider the evolution of the position of an ensemble of atoms that are exposed to an impulse of a periodic potential. This ''kick'' causes a focusing of atoms in time. There is a stage of strong focusing of some of the atoms, with a broad background of dispersed atoms. At a somewhat later time, however, there is a formation of a ''rainbow'' in the position distribution. At this stage there is very little confinement, but the method is then to apply a second kick. Another rainbow forms later in time, with a smaller overall dispersion. In principle, this feature can be made arbitrarily small by the application of an aperiodic sequence of kicks, leading to a strongly focused sample with essentially no background. In practice, it should be noted that backgrounds can also be caused by impurity atoms of the wrong atomic state or species, and by atomic motion on a substrate.

In the experiment, we observe the center-of-mass motion of cesium atoms exposed to a modulated one-dimensional optical lattice. With the proper choices of laser intensity and detuning from atomic resonance, the conservative optical dipole force can be significant while dissipative interactions are simultaneously minor enough to permit the study of coherent quantum dynamics. In the far-detuned limit, the atom remains in the ground state and its behavior is that of a point particle in an external potential [12]. The maximum well depth V_0 of the dipole potential (ac Stark shift) depends upon the light intensity, and the standing-wave interference pattern leads to the space-dependent potential $V(x) = V_0 \cos(2k_L x)$, where k_L is the wave number of the light. The light intensity is modulated as a series of short pulses at times $\{t_n\}$, with pulse shape function $F(t)$ [13]. The system is described by the Hamiltonian $\mathcal{H}(x, p, t) = p^2/(2m) +$

$V(x)\sum_n F(t-t_n)$. The strength of each kick is $\mathcal{E}\cos(2k_L x)$, where $\mathcal{E} \equiv V_0 \int_{-\infty}^{\infty} F(t)dt$.

To describe the focusing mechanism, let us examine the dynamics after a single kick at time $t_1 = 0$. The atoms undergo ballistic motion, where the spatial distribution transiently focuses. Initially stationary atoms near the potential minima experience a nearly harmonic kick and focus after a time $t_f = m/4k_L^2\mathcal{E}$. The distribution does not optimally focus at t_f because the potential produces aberrations similar to those occurring for focusing with a single, transversely broad standing wave. The spatial compression of the entire atomic distribution is characterized by the focusing factor $f_c \equiv \langle\cos(2k_L x)\rangle + 1$. This figure of merit is defined such that $f_c = 1$ for a uniform distribution, and $f_c = 0$ for a distribution completely localized at the potential minima. By minimizing f_c, we not only optimize the intensity of the central focus, but also reduce the undesirable background. The focusing factor minimizes at time Δt_1, shortly after t_f. If we apply a second kick at time $t_2 = t_1 + \Delta t_1$, the focusing factor f_c reaches a new minimum at time $t_3 = t_2 + \Delta t_2$. Generally, $\Delta t_{n+1} < \Delta t_n$ and $f_c(t_{n+1}) < f_c(t_n)$, as compression is iteratively increased while the time scale for focusing after subsequent kicks decreases.

The focusing mechanism is robust against the velocity spread along the standing-wave axis, where additional kicks will be required for a given degree of focusing at a higher temperature [11]. In a beam experiment, however, the longitudinal temperature would correspond to a spread in the relative kick timing, to which the system is sensitive. Accordingly, this method will not be effective for high-temperature thermal beams (without velocity selection). Low-temperature supersonic beams of atoms or molecules can be highly monochromatic in longitudinal velocity and are a more appropriate setting for this focusing method.

Our experimental apparatus is similar to that described previously [13–15]. We begin by collecting cesium atoms from background vapor in a standard magneto-optic trap (MOT) [16]. After collecting 10^6 atoms in 5 s, the atoms are loaded into a 3D, linearly polarized optical lattice that is tuned 18 GHz to the red of the Cs $6S_{1/2}$, $F = 4 \rightarrow 6P_{3/2}$, $F = 5$ cycling transition [17]. Once the atoms are confined in this lattice, both the MOT repumping light (tuned to the $6S_{1/2}$, $F = 3 \rightarrow 6P_{3/2}$, $F = 4$ resonance) and the current to the MOT quadrupole magnet coils are turned off. The atoms in the lattice are then cooled with a weak optical molasses for approximately 300 ms. After this cooling period, the 3D lattice is adiabatically extinguished so that the atoms trade their local confinement for a reduction in temperature. Finally, the atoms are exposed to a 50 μs pulse of repumping light to pump the atoms into the $6S_{1/2}$, $F = 4$ state. The 1D temperature along the focusing axis after optical pumping is approximately 700 nK.

The atoms are next exposed to the sequence of focusing kicks. The standing-wave consists of a retroreflected linearly polarized beam of light, again tuned 18 GHz to the red of the cycling transition. Each kick is nominally a 300 ns pulse of equal amplitude, gated through an acousto-optic modulator.

The free-space detection sequence begins at a variable time after the end of the focusing sequence when we apply a single, strong kick. This pulse is applied with the same beam that delivers the focusing kicks, but at a higher intensity and with a nominal duration of 600 ns. An electro-optic phase modulator (EOM) located between the atomic sample and the retroreflecting mirror is used to shift the phase of the standing wave at a time between the end of the focusing-kick sequence and the beginning of the detection pulse. Because of the nonzero response time of the EOM, the phase shift is fixed to begin 1 μs before the detection pulse begins. After the detection pulse, we measure the average momentum of the atomic distribution by allowing it to undergo ballistic expansion for 25 ms. The distribution is then frozen in an optical molasses and imaged in a 15 ms exposure on a charge-coupled device (CCD) camera. A new sample of atoms is loaded and focused for each measurement.

The state of an atom at the end of the focusing sequence is given by the state vector $|\psi_0\rangle$. The detection pulse is described well by the δ-function pulse operator $\hat{U}(\mathcal{E}_d, \phi) = \exp[-\frac{i}{\hbar}\mathcal{E}_d\cos(2k_L x + \phi)]$, where $\mathcal{E}_d$ and ϕ are the strength and the phase of the pulse [18]. The operators for detection pulses with phases of $\pm\pi/2$ may be abbreviated as $\hat{\mathcal{U}}_{(\pm)} \equiv \hat{U}(\mathcal{E}_d, \pm\pi/2)$. The average momentum after such a pulse is

$$\langle p_{(\pm)}\rangle = \langle\hat{\mathcal{U}}_{(\pm)}\psi_0|p|\hat{\mathcal{U}}_{(\pm)}\psi_0\rangle = \int \psi_0^*(x)\hat{\mathcal{U}}_{(\pm)}^*\left(\frac{\hbar}{i}\frac{\partial}{\partial x}\right)\hat{\mathcal{U}}_{(\pm)}\psi_0(x)dx$$
$$= \int \psi_0^*(x)\left(\frac{\hbar}{i}\frac{\partial}{\partial x} \pm 2k_L\mathcal{E}_d\cos(2k_L x)\right)\psi_0(x)dx = \langle p\rangle \pm 2k_L\mathcal{E}_d\langle\cos(2k_L x)\rangle. \quad (1)$$

From this analysis it results that the quantity

$$1 + \frac{1}{4k_L\mathcal{E}_d}(\langle p_{(+)}\rangle - \langle p_{(-)}\rangle) = 1 + \langle\cos(2k_L x)\rangle = f_c \quad (2)$$

is the focusing factor. In practice, we perform this measurement over a large ensemble of noninteracting atoms. To measure f_c, we kick the atoms with the standing-wave phase shifted by either $\pi/2$ or $3\pi/2$ and measure the average momentum as described earlier to find $\langle p\rangle_{(\pm)}$ and thus f_c. In the data that we present, the detection pulse fluence is $\mathcal{E}_d = 7.1\hbar \pm 10\%$. The uncertainty in this value is due to the calibration of the absolute laser intensity, the dominant source of uncertainty in the experiment.

Data from the experiment showing the time evolution of f_c after a single kick are shown in Fig. 1, for fluences $\mathcal{E}$ ranging over nearly an order of magnitude. The time Δt_1 at which the maximum spatial compression occurs and the degree of the compression are determined largely by $\mathcal{E}$. The values $\{\Delta t_n\}$ determined from plots of this type were used to empirically optimize the focusing-kick sequence and choose the times between successive kicks.

Besides the single-kick data, Fig. 1 also shows the results of quantum wave-packet-dynamics simulations, which exhibit good agreement with the data. We begin with an ensemble of identical wave packets uniformly spread out in x across the unit cell of the lattice. The wave packet momentum distribution is modeled as a sum of Gaussian and exponential components [13]. The three constants in this model were determined by self-consistently fitting to the data in Fig. 1 along with data from free-expansion temperature measurements. It is important to note that the initial state has a small but nonzero average momentum $\langle p\rangle/2\hbar k_L = 0.23 \pm 0.10$, which is likely due to an imbalance in the 3D lattice cooling system.

The simulations directly account for a number of known systematic effects in the experiment. The only correction prior to detection is for the nonzero duration of the focusing kicks. The most significant detection issue is that the EOM shifts the phase of the standing wave by only ~85% of the desired phase within the 1 μs allotted. This correction typically reduces the apparent compression by about 3.5%. We also account for the detection pulse duration, inhomogeneities in the imaging system [13], and the spatial extent of the atomic distribution that is convolved with the momentum distributions, each of which affect f_c by less than 1%. An ideal detection system is simulated by calculating $f_c = \langle\cos(2k_L x)\rangle + 1$ directly from the position-space wave function after the focusing kicks. This procedure typically results in a value of f_c less than 5% lower than that of the realistic system.

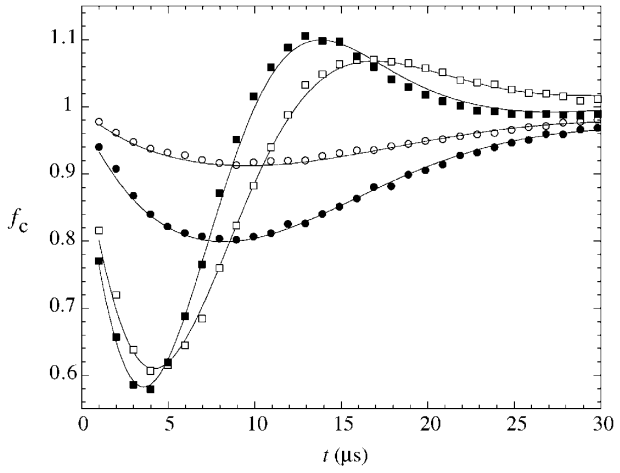

FIG. 1. Focusing behavior after one kick, for various kick strengths. The focusing factor $f_c = 1 + \langle\cos(2k_L x)\rangle$ is experimentally measured at various times for kick strengths $\mathcal{E} = 0.41\hbar$ (open circles), $\mathcal{E} = 1.03\hbar$ (filled circles), $\mathcal{E} = 3.09\hbar$ (open boxes), and $\mathcal{E} = 3.72\hbar$ (filled boxes). Also shown are the results of the quantum simulation for this system (solid lines).

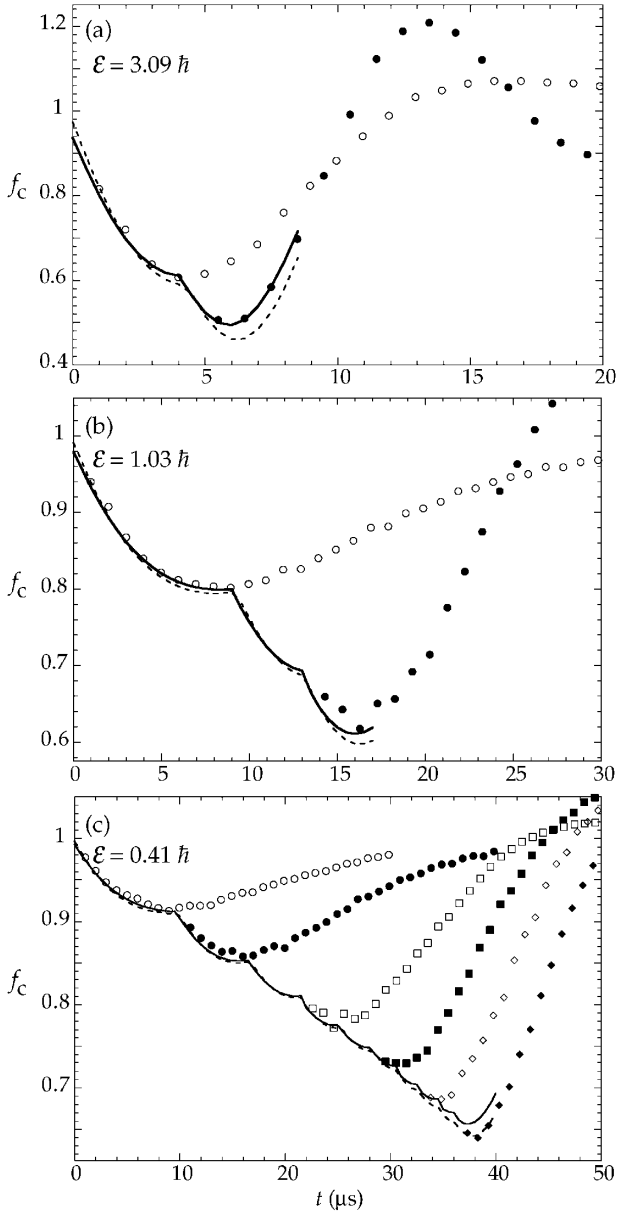

FIG. 2. Evolution of f_c after multiple kicks. The focusing factor f_c is measured (a) after one (open circles) and two kicks (filled circles) at $\mathcal{E} = 3.09\hbar$. For $\mathcal{E} = 1.03\hbar$ (b), data is shown after one (open circles) and three kicks (filled circles). For $\mathcal{E} = 0.41\hbar$ (c), the data are for one (open circles), two (filled circles), four (open boxes), six (filled boxes), eight (open diamonds), and ten kicks (filled diamonds). The results of the simulation are shown with (solid lines) and without (dashed lines) corrections for systematic detection effects.

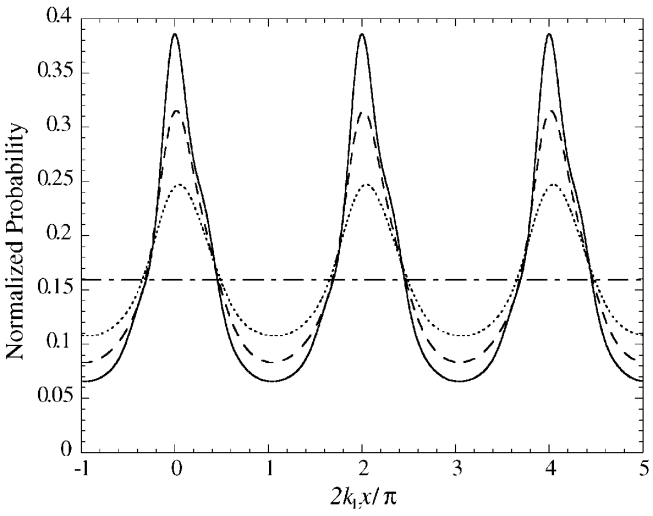

FIG. 3. Calculation of atomic focusing after multiple kicks: position distribution evolution. The evolution of the atomic spatial distribution is shown over several wells of the standing wave for the simulation shown in Fig. 2 with $\mathcal{E} = 1.03\hbar$. The initial condition (dot-dashed line) is spatially uniform. The distributions after one (dotted line), two (dashed line), and three (solid line) kicks are plotted at the time of maximum spatial compression, where f_c is minimized. The slight asymmetry is due to the nonzero initial average momentum of the atomic sample.

In Fig. 2, we present data from the measurements with iterative focusing. In each sequence, kicks were added until the time between successive minima became close to 1 μs, the slew time of the EOM. For $\mathcal{E}/\hbar = 3.09$, the sequence consisted of two kicks separated by 4.5 μs. For $\mathcal{E}/\hbar = 1.03$, the three-kick sequence had spacings of 9.4 and 3.9 μs. The ten-kick sequence with $\mathcal{E}/\hbar = 0.41$ had spacings of 10, 6.9, 4.7, 3.9, 3.0, 2.2, 2.1, 1.8, and 1.7 μs. Figure 2 also shows the results of simulations with the same parameters as those shown in Fig. 1, with and without the systematic detection effects. The difference between the two cases is comparable to the uncertainty in $\mathcal{E}_d$. In each case it is clear that the f_c is iteratively reduced with each kick. For weaker kicks, additional kicks are required to achieve equivalent compression.

To examine the focusing in another way, the position-space probability distributions from the simulation with $\mathcal{E}/\hbar = 1.03$ are plotted in Fig. 3. The trend of decreasing f_c with successive kicks appears here as an increase in the intensity of the focused features along with a corresponding suppression of the background. The degree of observed focusing is comparable to that which has been achieved in other experiments [6]. Note, however, that our kick sequence is limited by the response time of the free-space detection system. The focusing method is extensible to larger numbers of kicks and the fundamental limitation for focusing onto a substrate is the nonzero duration of the kicking pulses. As an illustration, the simulations with idealized detection were used to estimate the maximum focusing possible with 300 ns pulses. With $\mathcal{E}/\hbar = 1.03$, we find that $f_c < 0.25$ is feasible for a sequence of 18 kicks. Similar maximum compression is possible for sequences with the other values of $\mathcal{E}$, and higher compression is possible for shorter pulse durations.

This work was supported by the NSF, the R. A. Welch Foundation, the U.S. Israel Binational Science Foundation, the Sid W. Richardson Foundation, and the Fannie and John Hertz Foundation (D. A. S.).

*Present address: National Institute of Standards and Technology, Time and Frequency Division, MS 847, 325 Broadway, Boulder, CO 80305.
†Present address: Los Alamos National Laboratory, Theoretical Division (T-8), MS B285, Los Alamos, NM 87545.
‡Electronic address: raizen@physics.utexas.edu

[1] G. Timp, R. E. Behringer, D. M. Tennant, J. E. Cunningham, M. Prentiss, and K. K. Berggren, Phys. Rev. Lett. **69**, 1636 (1992).
[2] J. J. McClelland and M. R. Scheinfein, J. Opt. Soc. Am. B **8**, 1974 (1991).
[3] J. J. McClelland, R. E. Scholten, E. C. Palm, and R. J. Celotta, Science **262**, 877 (1993).
[4] Roger W. McGowan, David M. Giltner, and Siu Au Lee, Opt. Lett. **20**, 2535 (1995).
[5] R. Gupta, J. J. McClelland, Z. J. Jabbour, and R. J. Celotta, Appl. Phys. Lett. **67**, 1378 (1995).
[6] Special issue on *Nanomanipulation of Atoms*, edited by D. Meschede and J. Mlynek [Appl. Phys. B **70** (2000)].
[7] M. Mützel, S. Tandler, D. Haubrich, D. Meschede, K. Peithmann, M. Flaspöhler, and K. Buse, Phys. Rev. Lett. **88**, 083601 (2002).
[8] J. J. McClelland, R. Gupta, R. J. Celotta, and G. A. Porkolab, Appl. Phys. B **66**, 95 (1998).
[9] K. S. Johnson, J. H. Thywissen, N. H. Dekker, K. K. Berggren, A. P. Chu, R. Younkin, and M. Prentiss, Science **280**, 1583 (1998).
[10] I. Sh. Averbukh and R. Arvieu, Phys. Rev. Lett. **87**, 163601 (2001).
[11] M. Leibscher and I. Sh. Averbukh, Phys. Rev. A **65**, 053816 (2002).
[12] R. Graham, M. Schlautmann, and P. Zoller, Phys. Rev. A **45**, R19 (1992).
[13] D. A. Steck, V. Milner, W. H. Oskay, and M. G. Raizen, Phys. Rev. E **62**, 3461 (2000).
[14] D. A. Steck, W. H. Oskay, and M. G. Raizen, Science **293**, 274 (2001).
[15] W. H. Oskay, Ph.D. dissertation, The University of Texas at Austin, 2001.
[16] Steven Chu, Science **253**, 861 (1991).
[17] M. T. DePue, C. McCormick, S. L. Winoto, S. Oliver, and D. S. Weiss, Phys. Rev. Lett. **82**, 2262 (1999).
[18] L. E. Reichl, *The Transition to Chaos in Conservative Classical Systems: Quantum Manifestations* (Springer-Verlag, New York, 1992).